GEOPHYSICAL RESEARCH LETTERS, VOL. 24, NO. 19, PAGES 2423-2426, OCTOBER 1, 1997

Transient decreases of Earth's far–ultraviolet dayglow

L. A. Frank and J. B. Sigwarth

Department of Physics and Astronomy, The University of Iowa, Iowa City

Abstract. Ten years ago transient decreases in Earth's far–ultraviolet dayglow were reported for global images acquired with the high–altitude, polar–orbiting spacecraft Dynamics Explorer 1. These decreases were observed primarily in the atomic oxygen emissions at 130.4 nm. The diameters of these dark spots, or "atmospheric holes", were in the range of 50 to 100 km. Recently a sophisticated camera for imaging Earth's far–ultraviolet dayglow, with far greater spatial and temporal resolutions than its predecessor, was launched with the Polar spacecraft. The images from this spacecraft provide irrefutable evidence that these atmospheric holes are a geophysical phenomenon.

Introduction

The purpose of the present paper is to establish the existence of transient, spatially localized decreases of Earth's far–ultraviolet dayglow, or atmospheric holes, and to eliminate the possibility of instrumental artifacts. Images of Earth's dayglow from the camera on board the Polar spacecraft have sufficient spatial resolution to obtain multi–pixel images of the atmospheric holes. In addition the temporal resolution of the Polar camera is sufficient to image the motion of the same atmospheric hole in two consecutive frames.

Instrumentation and observations

The Polar spacecraft was launched on 24 February 1996 into an eccentric orbit with perigee and apogee altitudes of 5170 km and 50,510 km, respectively, an orbital period of 17.6 hours, and an inclination of 86°. The apogee is positioned over the Northern polar regions. The details of the design of the far–ultraviolet camera, i.e., the Earth Camera, that is part of the Visible Imaging System (VIS) for the Polar spacecraft are given by Frank et al. [1995]. This imager takes advantage of the spacecraft despun platform and stares at Earth with a field–of–view with dimensions of 20° × 20°. The filter passband is 124–149 nm for which the most prominent dayglow emission is that from atomic oxygen at 130.4 nm. An image intensifier that is serviced with a charge–coupled device (CCD) is used to obtain simultaneously accumulated responses in an array of 256 × 256 pixels. The angular dimensions of each rectangular pixel are 0.08° × 0.08°. The exposure times are programmable by ground command but are typically in the range of 12 s to 60 s.

Paper number 97GL02410.
0094-8534/97/97GL-02410$05.00

Images of the far–ultraviolet dayglow

One of the first global images of the dayglow that was available for our inspection is shown in Figure 1. The spacecraft altitude is 40,800 km and the geographic North latitude and East longitude are 82.4° N and 31.2° E, respectively. The only correction is the removal of easily identified ionization events in the CCD due to energetic charged particles. When the spacecraft is outside of the radiation zones then the numbers of such ionization events are in the range of 30 to 200 per image. These pixel responses are replaced by the respective medians of the adjacent pixels. The dayglow is shown for solar zenith angles ≤ 61.5°. At higher angles the sensor responses are often too low to securely identify an atmospheric hole. An example of an image with high solar zenith angles is given by *Frank and Sigwarth* [1997]. The linear dimension along the bottom of Figure 1 at Earth's surface is about 13,000 km. All dayglow images presented here are color–coded from low intensities of several hundred Rayleighs (faint, deep red) to highest intensities at about 15 kiloRayleighs (whitish yellow). The images presented in Figures 1, 5 and 6 were accumulated for 18 s and the responses of each of the 65,536 pixels were quasi–logarithmically compressed into eight bits. This quasi–logarithmic compression is linear from 0 to 63 DN (digitization numbers). For the range of sensor responses used in present paper the maximum error due to compression was 1 DN and not significant. The frame repetition time is 85 s.

The inset in Figure 1 displays an array of 15 × 15 pixels centered on the atmospheric hole. The range to the atmospheric hole, which is assumed to be positioned at an altitude of 500 km for the purposes of calculating coordinates [see Frank and Sigwarth, 1993], is 40,850 km and the corresponding geographic latitude and longitude are 62.3° N and 359.9° E, respectively. There is a smaller hole positioned midway between the box and edge of the dayglow on the right–hand side in Figure 1. The images shown in Figures 1 and 5 are interpolated between pixels using a two–dimensional linear algorithm which preserves any other features of the telemetered pixel array. Actual pixel values for the hole in the inset of Figure 1 are shown in the map of Figure 2. The corresponding spatial dimensions of each pixel are 57 × 57 km^2. Uncompressed DN are used throughout the paper. The mean digitization numbers, $\overline{DN}$, and the standard deviation σ are identified in the figure. The corresponding probability **P** that the atmospheric hole recorded in Figures 1 and 2 is a random event is once in about 3 × 10^{10} images. This probability **P** that a given cluster of contiguous darkened pixels is a random event is estimated with $P = m\,n\,! \prod_{i=1}^{n} P(<x_i)$ where m is the number of dayglow pixels in an image (typically 30,000 pixels), n is the number of darkened pixels in a cluster,

and P ($<x_i$) is the Gaussian probability for a decrease of x_i standard deviations or more from the mean value. The standard deviations and the means are determined directly from the images within adjacent pixel blocks or the same pixel block in a preceding or following image. At the lower right-hand corner of this pixel map there are two bright pixels. The brightening of these pixels is due to the charge deposited in these sites by the passage of an energetic charged particle. Whereas the darkened pixel clusters are securely identified as due to an object within the field-of-view the occurrence of a bright area that might be associated with impact into the upper atmosphere is compromised by the charges deposited by penetrating charged particles.

The statistical significance of the atmospheric holes can be further examined by systematically determining the mean and standard deviation σ for each of the 8,503 pixels in Figure 1. The methodology is straightforward. A block of 7 × 7 pixels is centered on the pixel to be tested. The mean and standard deviation are computed for the 32 pixels adjacent to the above pixel block. An inventory of all pixels with a given darkening of, for example, ≤ −2σ is acquired. This inventory is then searched for the frequency of occurrence of clusters with a given pixel population. This method is very direct and decisive in evaluating the Earth Camera images. The number of events with clusters of N adjacent darkened pixels, each ≤ −2σ, is shown in Figure 3 for the image in Figure 1. The atmospheric hole is clearly isolated from the randomly occurring clusters with lesser numbers of cluster members. The hole to the right of the box in Figure 1 is the event with 6 pixels in its cluster. Simple extrapolation of the distribution in Figure 3 (dashed line) to a 9-pixel cluster predicts that the maximum occurrence frequency for a randomly occurring 9-pixel event is once in every 300 images, whereas the atmospheric holes occur with a frequency of about once in each image for the usable frame size of Figure 1. Actually the probability of the random occurrence of this atmospheric hole is much less than that cited above because there are only 15 pixels with ≤ −3σ in the entire image of Figure 1 with 11 as single pixels and 4 pixels in the atmospheric hole. The probability that this is a random occurrence is extremely low when one considers that only 15 balls are available to randomly place 4 balls in 4 adjacent pockets of a grid of 8,503 pockets.

The application of a standard normal distribution can be also tested by computing the normalized probability of the occurrence of pixels with responses less than or equal to a given standard deviation. The results of this computation with the pixels shown in the image of Figure 1 are shown in Figure 4. The probabilities for the range of σ of interest here, −1.5 to −3.0, as shown in Figure 4 are well represented by the normal distribution. The somewhat larger probability at σ = −1 indicates that a Poisson distribution would be applicable at these values, as expected. The results shown in Figures 3 and 4 provide solid validation that the present statistical evaluations are accurate.

Another example of an atmospheric hole that is observed from lower altitudes is shown in Figure 5. The range from the spacecraft to the atmospheric hole is 20,040 km. The geographic latitude and longitude of the hole are 51.0° N and 25.4° E, respectively. The dimensions of each pixel are 28 × 28 km^2. The diameter of the atmospheric hole is in the range of 50 to 100 km. The probability P that the four darkest pixels alone are a random event is once in about 3 × 10^{11} images. This atmospheric hole is positioned above Poland.

The effects of "double vision" on the detection of atmospheric holes

Because the center of gravity of the Polar spacecraft is not positioned precisely on its spin axis the field-of-view of the camera executes a cyclic motion perpendicular to this spin axis with a period equal to that of the spin period of the spacecraft, i.e., 6 s. This motion of the field-of-view is parallel to the abscissas of the image frames presented here. The sample time per pixel is proportional to the projection of circular motion onto the image plane. This is well demonstrated by the subframe of the image of an ultraviolet star, Beta Chamaeleon (Right ascension, Declination = 12h 18', −79° 13'), shown in Figure 6(a). The star appears as two ansae separated by the amplitude of the angular motion of 0.38 degrees, or 4.6 pixels. This angular motion offers another opportunity to demonstrate that the atmospheric holes are not instrument artifacts. That is, for those occasional objects for which their apparent motion is nearly along the line-of-sight from the spacecraft, the image of the object should exhibit "double vision", or two darkened spots in the dayglow. Such a sighting is shown in Figure 6(b). This event occurs at solar zenith angles not shown in Figure 5 but in a limited sensor area which has enhanced sensitivity and thus provides statistically reliable responses. The range from the spacecraft to this atmospheric hole which occurred over Russia is 20,760 km with geographic latitude and longitude of 54.4° N and 91.5° E, respectively. The probability that the six darkest pixels is a random event is once in 1.5 × 10^7 images.

Two consecutive images of an atmospheric hole

Because the duration of the atmospheric holes is only ~90 s or less [*Frank and Sigwarth*, 1993], the frame repetition rate must be increased relative to that for the previously presented frames if detection of the same hole in two consecutive images is to be acquired. The frame rate was increased with the use of image compression techniques [*Frank et al.*, 1995]. The inaccuracies associated with this coding are small, 4 DN, which is the residual level set by ground command. The observed characteristics of the atmospheric holes are independent of whether or not the compression code is used. In addition the "double vision" due to the motion of the camera's field-of-view must be eliminated in order to achieve sufficient angular resolution to observe the hole in its early stage of expansion. The angular resolution was improved by using onboard knowledge of the spacecraft rotation phase and by employing the instrument's computers to back-bias (shutter) the sensor photocathode in order to sample only one of the ansae shown in Figure 6.

An example of the detection of the trail of the same atmospheric hole in two consecutive frames is shown in Figure 7. Shown are the two 12 × 12-pixel (750 × 750 km^2) subframes centered on the hole. The spacecraft position is 86.0° N and 260.0° E at an altitude of 45,300

Figure 1. A global view of Earth's far-ultraviolet dayglow at 1247:58 UT on 6 April 1996. The Earth's limbs are the curved boundaries of emissions at the left- and right-hand sides of the image. The times for all image frames are the beginning times for accumulation of sensor responses. A subframe shows the transient decrease in dayglow intensities known as an "atmospheric hole".

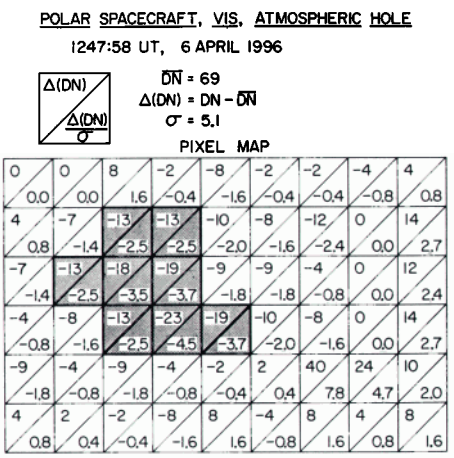

Figure 2. Pixel map for the atmospheric hole shown in the inset of Figure 1. DN is digitization numbers.

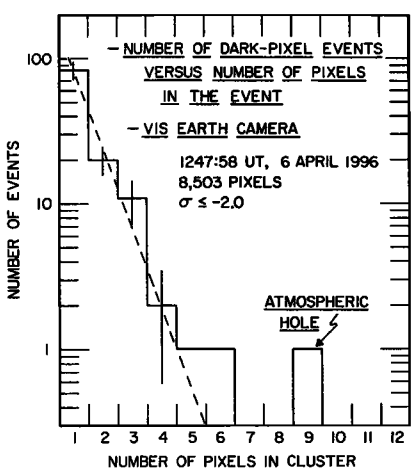

Figure 3. The number of dark-pixel events as a function of the number of adjacent darkened pixels in the event for the image shown in Figure 1.

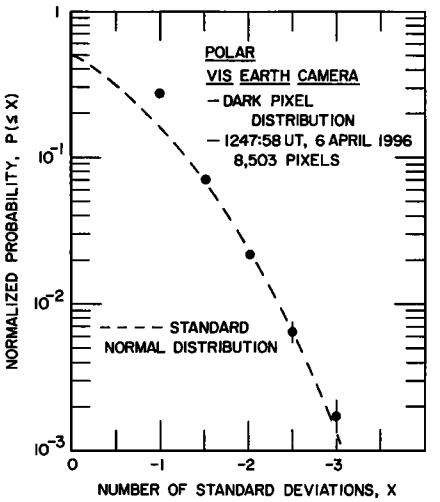

Figure 4. Comparison of the normalized probability for the occurrence of darkened pixels in Figure 1 as a function of standard deviation with a standard normal distribution.

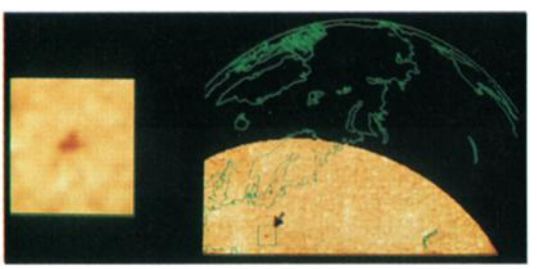

Figure 5. Image of Earth's ultraviolet dayglow at 0954:05 UT on 6 April 1996. A coastline map has been superposed upon the image in order to facilitate identification of the position of the event.

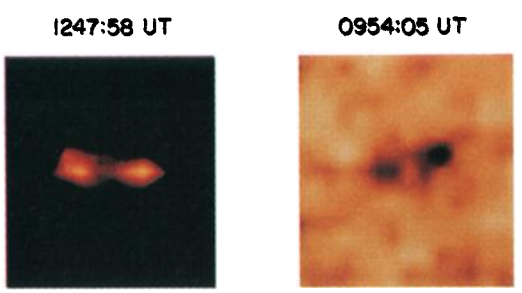

Figure 6. Two subframes that demonstrate the "double vision" that is expected for viewing real objects from misalignment of the center-of-gravity and spin axis of the spacecraft: (a) image of a star and (b) image of an atmospheric hole with velocity vector almost aligned with the line-of-sight.

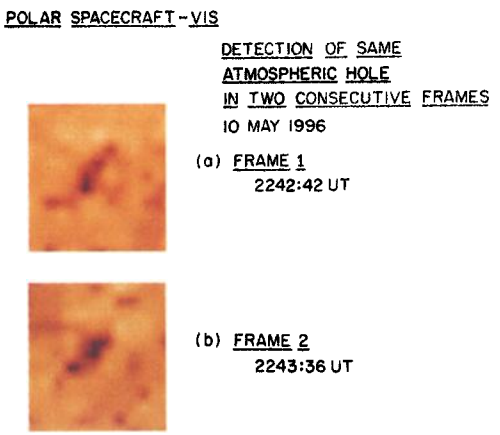

Figure 7. Subframes from two consecutive images. The same atmospheric hole is positioned in the centers of these subframes. The event occurs above the northern islands of Canada.

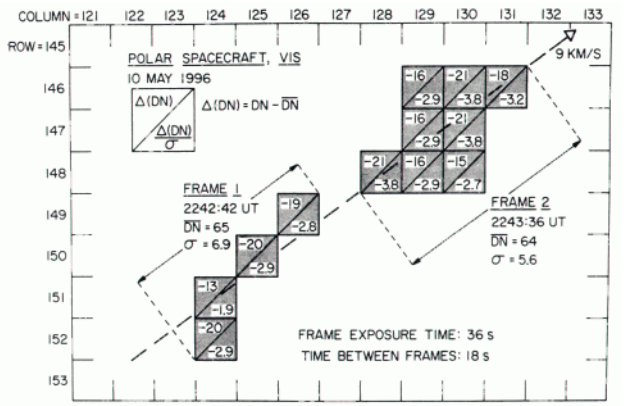

Figure 8. Pixel maps for the two sightings of a single atmospheric hole displayed in Figure 7. The motion is generally northward and from local evening to morning across the sunlit atmosphere. The apparent speed of the atmospheric hole is estimated from the length of the trail in Frame 2, i.e., about 9 km/s.

km at the beginning of the first frame. Spacecraft motion is slow and coordinates differ little for the second frame. At an assumed altitude of 500 km, the geographic coordinates of the atmospheric hole at the beginning of the first frame are 81.7° N and 250.2° E.

The identification of the two trails displayed in Figure 7 due to the motion of a single atmospheric hole is verified in Figure 8 by placing the two sets of darkened pixels into the column–row coordinates of the CCD array. Note that the darkened trails are the records of the motion and expansion of the object during the individual frame exposure times of 36 s. The pixel size at altitude 500 km as viewed from the spacecraft is 63 × 63 km^2. The two trails of darkened images are co-aligned to within the accuracy of about 1 pixel for removing the effects of angular motion of the field-of-view during a spacecraft rotation period. The gap between the two darkened pixel blocks is necessarily present because of the time interval between exposures. The lengths of the two trails are equal because the exposure times are the same. If the object consists of vapor, then its diameter is expected to increase. For example, these speeds are ~0.5 km/s for water vapor, and yield an increase in cloud diameter of ~1 km/s [*Frank and Sigwarth*, 1993]. Thus if the diameter is about 60 km at the beginning of Frame 1, then the time interval of ~60 s until Frame 2 will allow an increase in diameter to about 120 km, or a trail width of ~2 pixels. This is readily seen in the pixel map for Frame 2. Finally, the darkening of the pixels by 15 to 20 DN is explained by the fact that the object dwell time in each pixel as it travels across the camera's field-of-view is about 1/3 the frame time for the previously determined apparent speed of 10 km/s [*Frank and Sigwarth*, 1993]. Thus the expected signal is (1/3) (65–20) DN ≃ 15 DN where 20 DN is the equivalent zero level for the sensor electronics. These decreases are within 1σ of the observed values. Fulfillment of the above set of stringent conditions establishes that the detection of the same phenomenon in two consecutive images is robust. During the months of April through September when the Visible Cameras are not operating the frame rate for the Earth Camera is 54 s which is sufficiently fast to allow detection of the atmospheric holes in consecutive frames for at least 20% of the sightings.

On the frequency of atmospheric holes

During the 14 months of routine data acquisition beginning in early April 1996 approximately 400,000 global images of Earth's dayglow have been acquired. Typically one or two well-developed atmospheric holes with characteristics similar to the event shown in Figure 1 are found in each image. A reasonable estimate of the total number of atmospheric holes in these records is 500,000.

Our initial estimates for the frequency of detection of atmospheric holes are similar to the average frequency previously observed with the Dynamics Explorer-1 spacecraft during the period October 1981 through mid-January 1982 [*Frank and Sigwarth*, 1993]. These initial estimates for the global occurrence rates are in the range of 5 to 30 events/minute.

Summary

The VIS Earth Camera on board the Polar spacecraft is providing spatially resolved detections of these atmospheric holes as clusters of darkened pixels. These pictures of clusters of darkened pixels, the "double vision" of these clusters due to the motion of the spacecraft's camera platform, and the detection of trails of darkened pixels in consecutive frames provide undeniable evidence for atmospheric holes as a geophysical phenomenon.

Acknowledgments. This research was supported in part at The University of Iowa by NASA Contract NAS5-30316.

References

Frank, L. A. and J. B. Sigwarth, Atmospheric holes and small comets, *Rev. Geophys., 31*, 1–28, 1993.

Frank, L. A. and J. B. Sigwarth, Detection of atomic oxygen trails of small comets in the vicinity of Earth, *Geophys. Res. Lett.*, (this issue), 1997.

Frank, L. A., et al., The visible imaging system (VIS) for the Polar spacecraft, *Space Sci. Rev., 71*, 297–328, 1995.

L. A. Frank and J. B. Sigwarth, Department of Physics and Astronomy, The University of Iowa, Van Allen Hall, Iowa City, IA 52242. (e-mail: frank@iowasp.physics.uiowa.edu; sigwarth@iowasp.physics.uiowa.edu)

(Received March 31, 1997; revised July 28, 1997; accepted July 28, 1997.)